Reconstructed Kinematics and Hydrodynamic Loading Using Spray Root Propagation in Wedge Water Entry

Journal:	*SNAME Maritime Convention 2020*
Manuscript ID	SMC-010-2020.R2
Submission Type:	Technical Paper - Peer Reviewed
Keywords:	slamming, fluid-structure interaction, spray root

SNAME Maritime Convention 2020
29 September – 2 October, Houston TX

www.sname.org

Reconstructed Kinematics and Hydrodynamic Loading Using Spray Root Propagation in Wedge Water Entry

M. Javad Javaherian (SM), **Zhongshu Ren** (SM) and **Christine M. Gilbert** (M)
Kevin T. Crofton Department of Aerospace & Ocean Engineering, Virginia Polytechnic Institute and State University, Blacksburg, VA

Wedge water entry studies are often performed by Naval Architects to estimate hydrodynamic pressure loads on small craft operating in waves. There are a number of theoretical formulations that have been developed in an effort to simplify the process of estimating design loads for vessel design. The work presented in this paper is the first step toward using a theoretically-based tool to reconstruct hydrodynamic pressures by taking spray root position measurements. This paper shows the validity of this method using a case study of a rigid wedge drop experiment. Future components of this work will further develop this tool to be used for highly-flexible structures and also in-situ pressure measurements at sea. The results of this paper show that the Wagner (1932) reconstruction method predicts the residual hydrodynamic pressure due to the fact that the theory considers the effects of acceleration. Meanwhile, the Armand and Cointe (1986) reconstruction method shows that the peak pressure magnitude and location can be reasonably predicted.

KEY WORDS:

hydroelasticity; wedge drop; spray root

INTRODUCTION

Wedge water entry is one of the well-known problems for naval architects, especially those who work on the design of high-speed vessels. Over the years, many researchers, to be discussed in upcoming paragraphs, have developed models to simulate a prismatic wedge impacting the water surface, which can be applied to a vessel traveling in waves. Since slamming can tangibly influence the structural strength, overall performance and crew functionality on board, accurate prediction of slamming loads is an indispensable step in the design process of planing vessels. Moreover, there has been a growing interest to implementing the wedge water entry results into predicting the motions of the planing hulls, using 2D+t method (Faltinsen (2005)). This method relates the problem of the motion of a prismatic planing vessel into problem of a 2D wedge that vertically enters into the water. Once the hydrodynamic loading problem of the 2D wedge is solved, results can be used in order to predict the motion and loads on high-speed planing vessel.

It is shown in the literature that as the wedge with a deadrise angle of β penetrates into a calm water, i.e. in Fig. 1, the disturbance generates water pile up and the spray root, which is the point of maximum curvature on the water surface. Researchers have studied the relationship between spray root, kinematics and hydrodynamic loading. The problem was first introduced by von Karman (1929) for the application of the design of the seaplane landing on a water surface. A more justified model was then suggested by Wagner (1932), where he employed asymptotic theory to relate the wedge water entry problem to an expanding flat plate. Even though his model predicts better results for the impact pressure compared to the von Karman (1929) model, there exists a singularity in the governing equation for the hydrodynamic loading at the location of the spray root. Further researchers tried to develop new models so that they could solve the singularity problem and estimate more accurate results for a wide range of deadrise angles. Logvinovich (1969); Armand and Cointe (1986); Vorus (1996); Mei et al. (1999) and Judge et al. (2004) are some examples for these studies. Wagner (1932), Generalized Wagner, Logvinovich (1969), and Armand and Cointe (1986) will be adapted and used in this study and will be discussed in more detail in the next section.

The wedge water entry problem has also been examined experimentally in addition to analytically and numerically. Zhao and Faltinsen (1993) proposed a numerical model and carried out a series of experiments to validate their model. These tests covered a wedge and also a bow flare section. They compared free surface profile, pressure coefficient, slamming force, and penetration speed between the experiment and model predictions. Yettou et al. (2006) conducted a series of experiments to parametrically investigate the wedge free fall water entry. Effects of drop height, deadrise angle, and wedge mass on the impact pressure were studied. In addition, some non-dimensional analysis was also discussed. Lewis et al. (2010) performed some experiments on water entry of a 25° deadrise-angle wedge and measured the

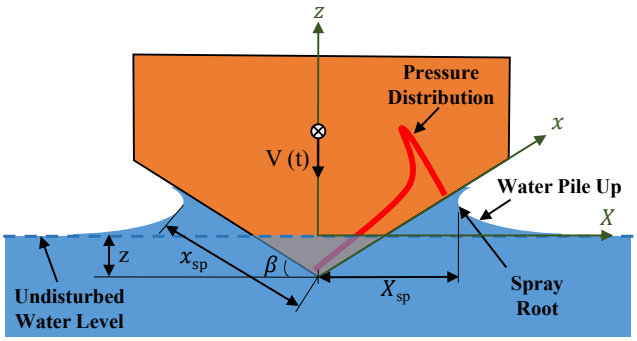

Figure 1: A schematic depicting the vertical water entry of a wedge.

kinematics and pressure-time history of the wedge during the impact. They also made attempts to visualize the fluid flow around the wedge to study the effect of the spray root on the exerted hydrodynamic pressure.

The studies mentioned to this point are on rigid wedge impact. Attention is now given to studies of flexible wedge water entry. Korobkin et al. (2006); Qin and Batra (2009); Panciroli and Porfiri (2015) developed separate models to study the water entry of a flexible wedge. In their models, they investigated the effect of the hydrodynamic loading on the structural response of the model.

Experimentally, water entry of a compliant wedge was studied by Panciroli and Porfiri (2015). They used particle image velocimetry (PIV) to evaluate the effects of flexibility on the hydrodynamic loading and structural response of the flexible panels. They compared the experimental results with their semi-analytical model. Shams et al. (2017) also experimentally investigated the water entry and exit of a flexible wedge. They used PIV measurements to obtain the velocity and pressure field around the wedge. They also studied free surface elevation to compare these experimental results with their semi-analytical model for slamming.

Ren et al. (2018, 2019); Javaherian et al. (2019) conducted several experiments to investigate the interaction between hydrodynamic loading and the structural response of a flexible wedge. They implemented Stereoscopic-Digital Image Correlation (S-DIC) to measure the displacement and also out-of-plane deflection of the wedge during the impact. Javaherian et al. (2019) introduced a novel method for tracking and measuring the spray root propagation along the bottom of a flexible wedge. Having fully synchronized measurements, they studied the interaction between the spray root, hydrodynamic loading, and structural response of the wedge. Fisher et al. (2019) proposed a two-way coupled, low fidelity, semi-analytical approach to simulate water entry of a flexible wedge. The coupling relates the spray root location in the fluid to the deflection on the wedge panel in contact with the water. Results showed a very good agreement with experimental results presented by Javaherian et al. (2019) and Ren et al. (2019).

Due to the expanded use of composite materials in high-speed vessels as well as the need to increase speed and decrease vessel weight, the vessel structure can no longer be considered rigid. As previously mentioned, it is important to have an accurate estimation of the design loads a high-speed vessel will encounter to increase the operational envelope. Use of the established theoretical models for rigid wedges in this context results in uncertainty for flexible wedges since they were not designed to take into account these physics. The approach of this paper is to allow for a semi-empirical prediction of the pressure distribution on the bottom of a wedge due to free-fall by inputting the spray root into existing theoretical models. This approach is important for two reasons: (1) for experiments on highly flexible structures, it is not possible to use traditional pressure sensors as they cause stiffening of the bottom plate that would not normally be present, and (2) an approach that allows for in-situ measurements in the field can be desirable.

In this paper, a new technique is proposed to reconstruct the wedge kinematics and exerted hydrodynamic pressure on the wedge water entry problem using the spray root time-history as an input into existing theoretical models. A case study will be presented in this paper, wherein the proposed reconstruction method will be used for a rigid wedge experiment. The reconstructed results from this method will be compared to both the full experimental measurements as well as the full theoretical prediction. The methodology developed and presented in this paper is the first step to reconstruct the hydrodynamic pressure and structural response in water entry of highly flexible structures in the context of both the water entry problem and a vessel traveling through waves.

METHODOLOGY

In this body of work, existing theoretical models that have been developed to predict pressures for vertical rigid wedge water entry will be adapted to take the spray root position at each time step to output the resulting pressure on the wedge. The intent of the original theoretical models was to use an impact velocity and acceleration to determine the hydrodynamic pressure distribution and wedge kinematics at all subsequent times. The two long-term goals of this project are to (a) incorporate spray root measurements for a highly-flexible wedge, and (b) use spray root measurements on a high-speed planing vessel in waves to compute accurate hydrodynamic pressure distributions. The work in this paper will establish this method for a rigid wedge by using the following models: (1) Wagner (1932), (2) Generalized Wagner as presented in Zhao et al. (1996), (3) and (4) Logvinovich and modified Logvinovich as presented in Korobkin (2004), and (5) Armand and Cointe (1986). Of these five models presented, all but Wagner (1932) are formulated for constant entry velocity. Wagner (1932) was formulated for non-constant entry velocity. Later work on the development of this method will be to re-derive models (2) to (5) to consider non-constant entry velocity.

Wagner Model

Wagner (1932) used asymptotic theory to collapse the 2-D wedge problem to an expanding line-boundary value problem that must be solved at each timestep. The extent of the line, for a symmetric wedge, is $-X_{sp}(t)$ to $X_{sp}(t)$, where $X_{sp}(t)$ is the instantaneous location of the intersection of the body with the free surface. Outside of this domain, the free surface kinematic boundary condition states that all particles on the free surface must remain on the free surface, so the velocity potential, ϕ, at all X locations outside of the line must be equal to zero. In this model, the body remains fixed, and the fluid flows upward. The velocity of the fluid is the magnitude of the velocity of the wedge, but in this frame of reference travels upward. The remaining models that will be discussed in this paper have a similar basis to this model. Furthermore, the relationship between the vertical position of the wedge and the spray root location,

$$z = \frac{2}{\pi} X_{sp} \tan\beta, \tag{1}$$

will be used for all models. The differences between each subsequent theoretical model and the present one will be noted in the following subsections.

Using potential flow theory, the function for the velocity potential can be solved, and the pressure distribution can be solved using Euler's equation with the assumption that the fluid acceleration is the dominant term in Euler's equation. Finally, there was a small angle assumption made for the deadrise angle. The final result for the hydrodynamic pressure is:

$$p(X) = \frac{1}{2}\rho V^2 \left[\frac{\pi}{\beta} \frac{X_{sp}}{\sqrt{X_{sp}^2 - X^2}} - \frac{X^2}{X_{sp}^2 - X^2} + \frac{2\ddot{z}}{V^2}\sqrt{X_{sp}^2 - X^2} \right]. \tag{2}$$

It is noted that there exists a singularity at the location of the spray root, $X = X_{sp}$, in the formulation as observed in Eq. 2. The pressure equation is only valid from the range $-X_{sp}(t) < X < X_{sp}$, and this model cannot predict the pressure at and beyond the spray root location.

It is worthwhile to mention that once the pressure data are reconstructed on the X-axis using these formulations, the results are then transformed back to the x-axis so they can be comparable with the experimental pressure measurements (see Fig. 1). The process of transformation is repeated for all other theoretical models that are covered in this study.

Generalized Wagner Model

The Generalized Wagner method was presented by Zhao et al. (1996). The main differences between the Generalized Wagner and Wagner (1932) include: (1) all other terms in Bernoulli's equation were retained except for the hydrostatic pressure, (2) the deadrise angle was allowed to be larger (no small angle approximation was used), and (3) the velocity was assumed to be constant. The hydrodynamic pressure distribution in this model is summarized as:

$$p(X) = \frac{1}{2}\rho V^2 \left[\frac{\pi}{\tan\beta} \frac{X_{sp}}{\sqrt{X_{sp}^2 - X^2}} - \cos^2\beta \frac{X_{sp}^2}{X_{sp}^2 - X^2} - \sin^2\beta + 2 - \pi \right]. \tag{3}$$

Again, it can be seen that there exists a singularity at the location of the spray root, $X = X_{sp}$, in the formulation as observed in Eq. 3, and the formulation is only valid up to the spray root location.

Original and Modified Logvinovich Models

The original Logvinovich (1969) method is similar to Wagner (1932), except that the small deadrise angle assumption is not used in the first term, and the entry velocity is assumed constant. The simplified version of the Logvinovich (1969) formulation for the hydrodynamic pressure in the contact region is presented by Korobkin (2004):

$$p(X) = \frac{1}{2}\rho V^2 \left[\frac{\pi}{\tan\beta} \frac{X_{sp}}{\sqrt{X_{sp}^2 - X^2}} - \frac{X_{sp}^2}{X_{sp}^2 - X^2} \right]. \tag{4}$$

If the second order terms with respect to wedge deadrise angle, β, are retained so that the small deadrise angle assumption is not applied, then the Modified Logvinovich model is obtained (Korobkin (2004)) as shown below:

$$p(X) = \frac{1}{2}\rho V^2 \left[\frac{\pi}{\tan\beta} \frac{X_{sp}}{\sqrt{X_{sp}^2 - X^2}} - \cos^2\beta \frac{X_{sp}^2}{X_{sp}^2 - X^2} - \sin^2\beta \right]. \tag{5}$$

Again, one can notice from the Eqs. 4 and 5 that both of the Original and Modified Logvinovich models have singularity at the location of the spray root, $X = X_{sp}$, and the formulation can only be used to compute the hydrodynamic pressure inside the wetted area of the body.

Armand & Cointe Model

Armand and Cointe (1986) resolved the singularity issue in the hydrodynamic pressure prediction by using a piecewise formulation for the pressure. This involves matching the inner domain (inside the jet) solution with the outer domain (outside the jet) solution. These two formulations are linked together by matching the jet thickness on both sides of the singularity. The pressure distribution from Armand and Cointe (1986) model in the outer domain, $X < X_{sp}$, is written out by Zhao and Faltinsen (1993) through using the Bernoulli equation as:

$$p_{out} - p_0 = \rho V X_{sp} \frac{dX_{sp}}{dt}(X_{sp}^2 - X^2)^{-\frac{1}{2}} -$$
$$\rho V X_{sp} \frac{dX_{sp}}{dt}[2X_{sp}(X_{sp} - X)]^{-\frac{1}{2}} + 2\rho \left(\frac{dX_{sp}}{dt}\right)^2 |\tau|^{\frac{1}{2}}(1 + |\tau|^{\frac{1}{2}})^{-2}, \quad (6)$$

and in the inner domain, $X \geq X_{sp}$, the pressure can be computed using:

$$p_{in} - p_0 = 2\rho[dX_{sp}/dt]^2 |\tau|^{\frac{1}{2}}(1 + |\tau|^{\frac{1}{2}})^{-2}, \quad (7)$$

where $|\tau|$ should be computed at each time step using the transcendental relationship:

$$X - c = (\delta/\pi)(-\ln|\tau| - 4|\tau|^{\frac{1}{2}} - |\tau| + 5), \quad (8)$$

where δ, the jet thickness, can be obtained from:

$$\delta = \pi V^2 \, 2X_{sp}[4dX_{sp}/dt]^{-2}. \quad (9)$$

Once the δ is known for each time step from Eq. 9, τ has to be computed numerically from Eq. 8. Finally, the hydrodynamic pressure can be determined using both Eqs. 6 and 7. The entry velocity is still assumed constant for the derivation of this model. This might cause some uncertainty to the analysis, where the solution is considered for a free-fall wanter entry problem.

Traditional Approach and Proposed Approach

When using the theoretical formulations described in the previous subsections, the spray root location using Eq. 1, and the impact velocity, V, is specified. The pressure data is then predicted using the equations for pressure, given as Eqs. 2 to 7. Although these methods provide a good estimation for the pressure distribution, there exists some discrepancies between the predicted values and the actual measurements due to simplifications that were made when deriving the theoretical equations. Once the pressure distribution is computed and integrated to determine the total force on the body, the rigid body kinematics can be computed.

In this study, a modified method of adapting these theoretical models is implemented. The experimental spray root position is used as an input into the equations for hydrodynamic pressure (Eqs. 2 to 7). Once the pressure distribution is computed, then the kinematics of the wedge can also be computed. The differences in the calculation method are shown in Fig. 2, where the traditional method is shown on the left and the proposed method is shown on the right. In the traditional method, the calculation is looped through time using updated velocity information. Using the proposed empirical method, a new spray root position and velocity is taken to reconstructed pressure at each time. The goal of this new approach is that the method be extended to provide accurate predictions of pressure on highly flexible structures and vessels operating in waves.

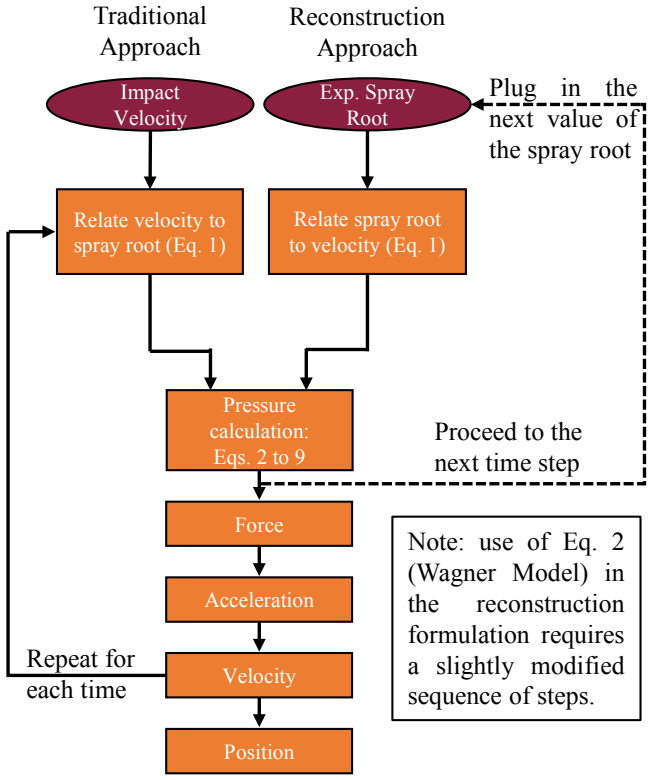

Figure 2: Flowchart demonstrating the traditional method for following the theoretical formulations (left side) and the proposed method (right side).

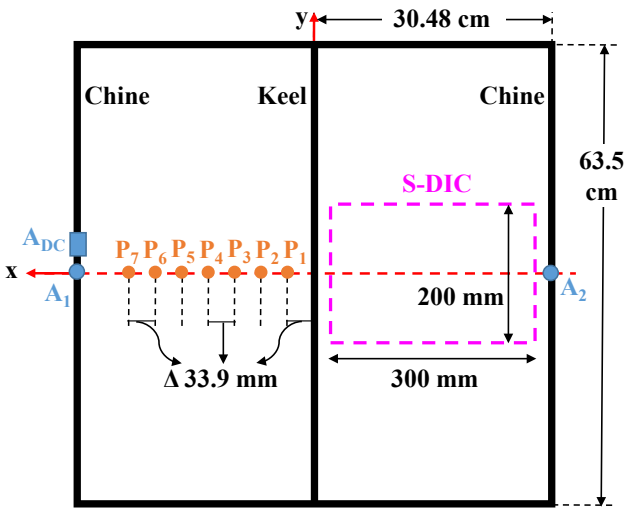

Figure 3: Plan view of the wedge showing the dimensions of the wedge and locations of the sensors. (Image courtesy of Javaherian et al. (2019)).

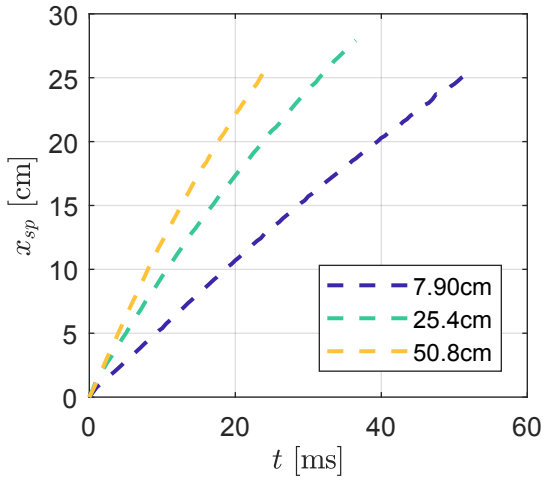

Figure 4: Spray root propagation on the bottom of the wedge for different drop heights. (Figure regenerated from Javaherian et al. (2019)).

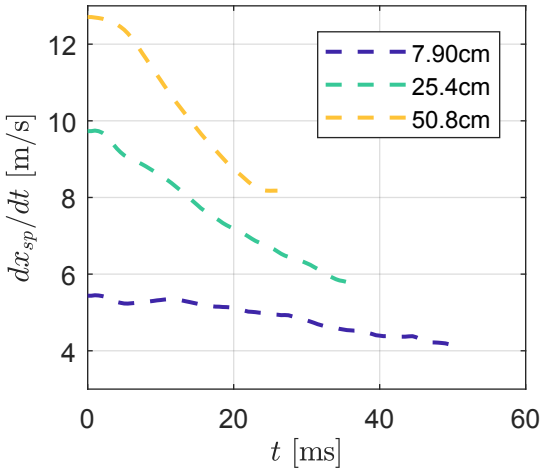

Figure 5: Spray root speed on the bottom of the wedge for different drop heights.

CASE STUDY

To show a demonstration of the new proposed method, a case study is presented using experimental data from Javaherian et al. (2019). In this experimental study, spray root, hydrodynamic pressure, and rigid body kinematics were measured. For the work presented in this paper, the spray root information is used as the input into the theoretical models, as shown in Fig. 2. Since the wedge kinematics and hydrodynamic pressure were also measured, these experimental measurements can then be compared to the results of the new reconstruction method. Finally, the theoretical model predictions for hydrodynamic pressure (shown as the traditional method in Fig. 2) will also be compared with the experimental measurements and the new approach.

Experimental Setup

The exact details of the experiment from this case study can be found in Javaherian et al. (2019); Ren et al. (2019). The rigid aluminum wedge model with a deadrise angle of $\beta = 20°$ is used in this case study. Fig. 3 shows the locations of all the sensors used in the experiment as seen from the top view. A string potentiometer was used to measure the position time-history of the wedge during the experiments. The vertical impact acceleration of the wedge was recorded by three accelerometers that were mounted on both sides of the wedge (A_1, A_2 and A_{DC}). An array of seven pressure transducers were mounted on the bottom of the wedge to measure the hydrodynamic loading during the water impact. All sensors were located within increments of 33.9 mm at one side of the wedge bottom, as it is shown in Fig. 3. The x-direction is called the characteristic line. The pressure measurements were sampled at a sampling rate of 200 kHz. Spray root measurements were taken using high-speed photography with 2000 fps and digital image processing to quantify the spray root evolution. Fig. 4 shows the spray root propagation on the wedge bottom for different drop height, H = 7.9, 25.4 and 50.8 cm (corresponding to impact velocity of V_0 = 1.219, 2.175 and 3.057 m/s, respectively). The spray root propagation speed for these drop heights is also plotted in Fig. 5. The spray root propagation speed was computed by taking the time-derivative of the spray root position-time history. These results are taken from Javaherian et al. (2019) and are the inputs that are taken in the proposed method.

RECONSTRUCTION ANALYSIS

In this section, results of the reconstruction technique will be reported and will be compared to pure theory and pure experiment. First, the hydrodynamic pressure distribution will be presented and discussed. The discussion of an empirical scaling will presented for the Armand and Cointe (1986) model. Following this will be the presentation and discussion of the pressure time histories compared at experimental pressure sensor locations. Finally, the reconstructed kinematics will be presented and discussed. It is noted that because the kinematics are dependent upon the hydrodynamic pressure, the focus of this section shall be on the hydrodynamic pressure.

Reconstructed Pressure Distribution

Pressure data reconstructed from different theoretical models using experimental spray root data for V_0 = 1.219 m/s are depicted in Fig. 6. Results are shown as spatial distribution in different time steps that correspond to the time in which sensors P_1 to P_7 reach their peak. Results show that the reconstructed pressure data from Armand & Cointe and also Logvinovich models predict better results compared to the other models. These models can reasonably predict the peak location and magnitude, specially in early time steps. However, as the time passes. The tail of the pressure, say the residual pressure, predicted by these methods experience a lower loss compared to the experimental results.

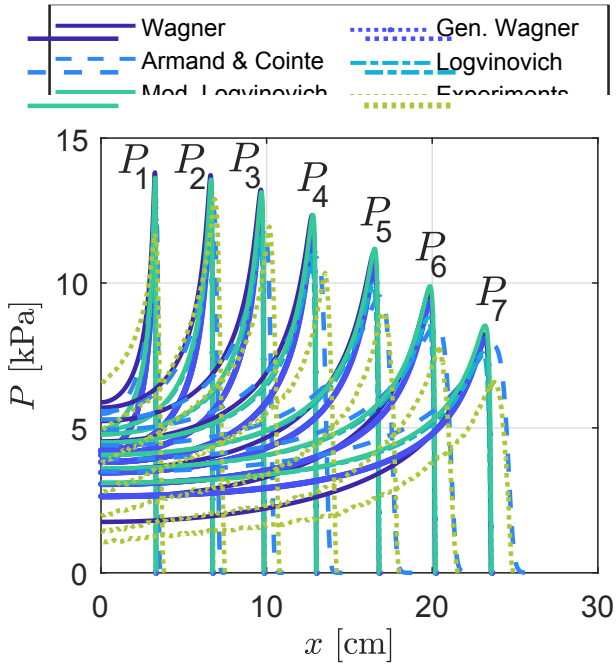

Figure 6: Pressure Reconstruction from different models for the impact velocity of V_0 = 1.219 m/s. Each curve denotes the time, in which the corresponding sensor reaches the peak. These time steps are t = 6 ms, t = 12.5 ms, t = 18.5 ms, t = 25 ms, t = 32.5 ms, t = 40 ms and t = 48 ms for the sensors P_1 to P_7, respectively.

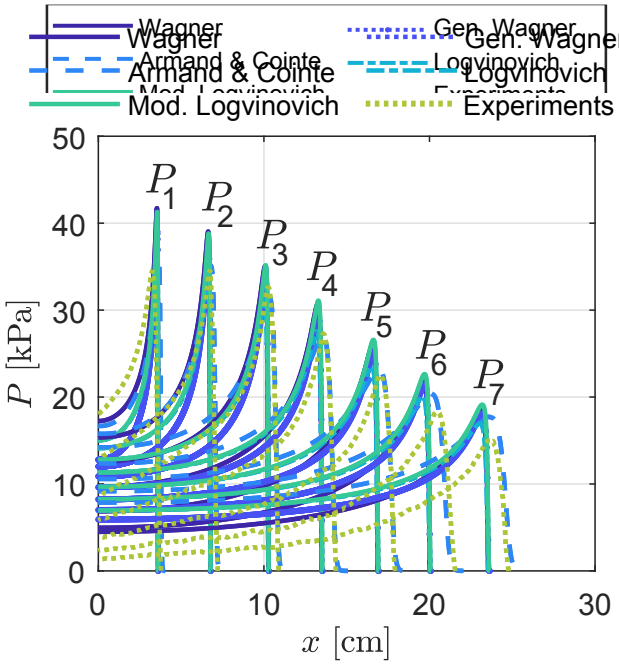

Figure 7: Pressure Reconstruction from different models for the impact velocity of V_0 = 2.175 m/s. Each curve denotes the time, in which the corresponding sensor reaches the peak. These time steps are t = 3.5 ms, t = 7 ms, t = 11 ms, t = 15 ms, t = 19.5 ms, t = 24 ms and t = 29.5 ms for the sensors P_1 to P_7, respectively.

Fig. 7 illustrates the similar results for the reconstructed pressure corresponding to the impact velocity of V_0 = 2.175 m/s. Results plotted as spatial distribution in different time steps, each of which representing the time that the sensor reaches the peak. For a better view of how these models compare, please see Fig. 8 (a) and (b), which show a closer look at t = 11 and 19.5 ms. The comparison also shows that the reconstructed pressure data from the Armand & Cointe and also Logvinovich models predict better results compared to the other models. The peak location and the corresponding magnitude are acceptably predicted by these models, specially in early time steps. Nonetheless, the tail of the pressure is reconstructed higher than the experimental values for the last 3 time steps. One possible reason is that these models are developed based on a constant entry speed. Even though using experimental spray root results can compensate for this to some extent, the residual peak pressure stays higher than the experimental values for the later time steps.

Fig. 9 quantitatively compares the magnitude and the location of the peak pressure reconstructed from each model with the experimental results. These values are plotted versus location of the sensors for V_0 = 2.175 m/s.. The comparison in Fig. 9a shows that Armand & Cointe model can predict the location of the peak very well. The error for the peak location is less than 2% for this method. As far as the magnitude of the peaks is concerned, Fig. 9b shows the Armand & Cointe model predicts the magnitudes to within 6% except at the locations of P_6 and P_7. For the last two sensors, the error is 10% and 17%, respectively. In fact, for the last two sensors, the deviation becomes greater for all reconstruction methods. Comparison also shows that after the Armand & Cointe method, the Logvinovich model results in better reconstructed pressure data compared to the remaining methods. The Generalized Wagner, Modified Logvinovich and original Wagner method predict the results with much higher deviations.

Comparison Between Traditional and Reconstructed Approach

In Fig. 2, the reconstruction approach that was used in this study was also compared with the traditional approach. To verify the reconstruction approach, the study has been repeated using the traditional approach for all the above-mentioned theoretical models. Results are compared to the reconstructed pressure to gauge the validity of the reconstruction technique and evaluate the effectiveness of using this semi-empirical approach. Fig. 10 to 14 show a comparison of the pressure distribution from pure theory (traditional approach), reconstruction method (subject of this paper), and pure experiments. These highlight the improved accuracy of these models. This is especially evident for the first two sensors, P_1 and P_2 in all models. Comparing the peaks resulted by the Generalized Wagner theory in Fig. 10, one can observe that the peak of sensor P_1 is computed to be 32% higher

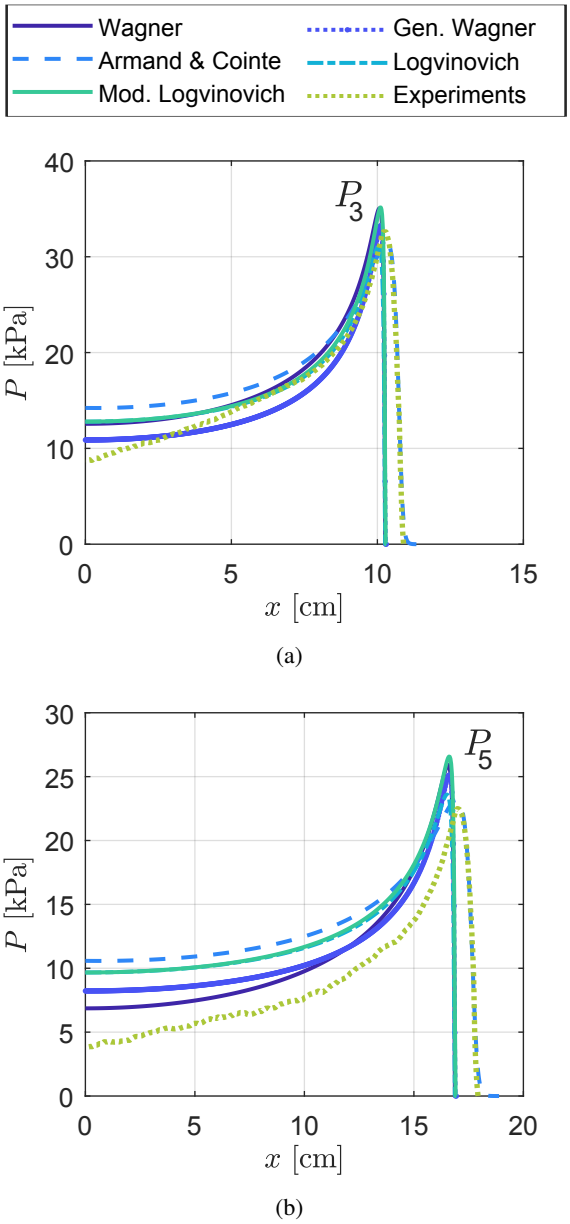

Figure 8: Pressure Reconstruction from different models at (a) t = 11 ms and (b) t = 19.5 ms.

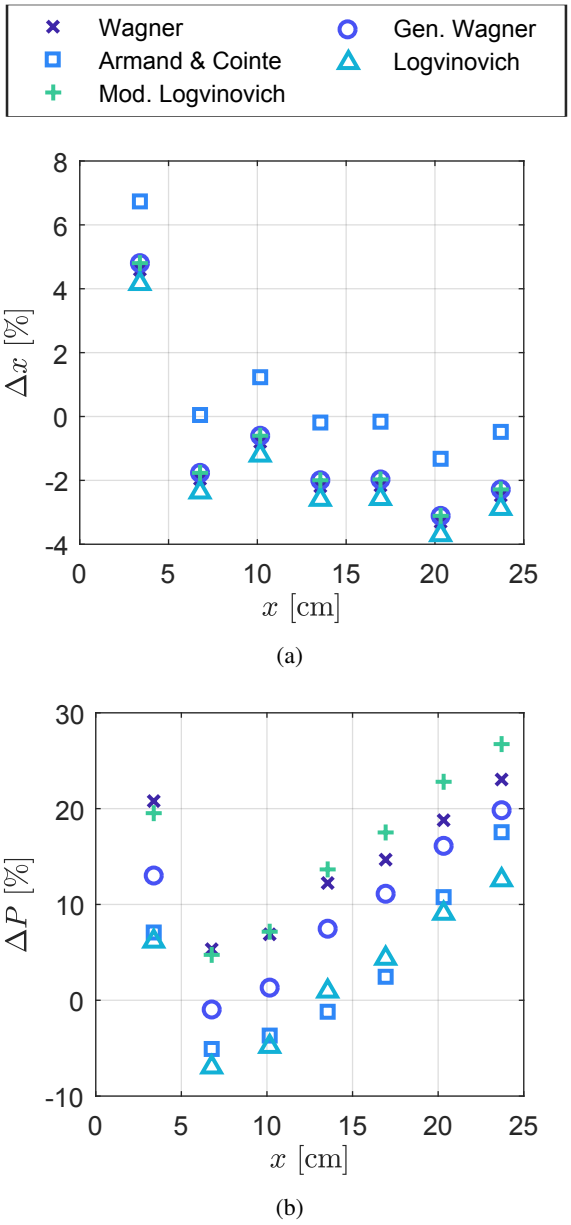

Figure 9: Comparison between (a) location and (b) magnitude of the peak pressure reconstructed from different models with the experimental results for V_0 = 2.175 m/s

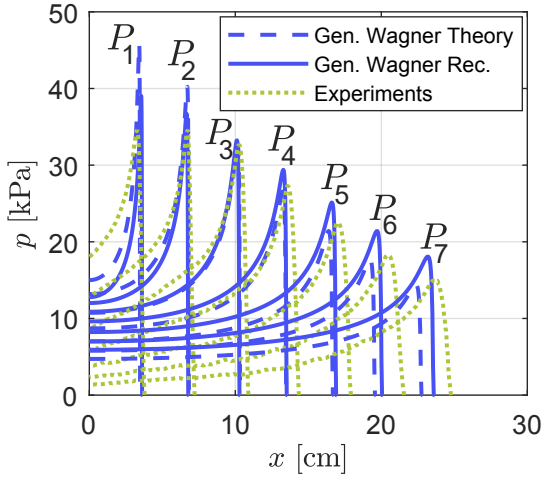

Figure 10: Spatial pressure distribution resulted from the traditional (theory) and the reconstruction approach using the Generalized Wagner model for $V_0 = 2.175$ m/s. Results are compared with the experimental pressure distribution. The curves correspond to the time steps that were presented in the Fig. 7.

than the experimental peak. For the reconstruction approach, this deviation is reduced to 12%.

Additionally, the reconstruction technique predicts the location of the peaks more accurately compared to the traditional approach for all models. For example, the error of the location of the peak corresponding to the P_7 in Fig. 11 is estimated to be within 8% by the Logvinovich theory, but to within 2% using the reconstructed approach for this model.

Among the traditional models, it is observed that the residual pressure predicted by the Wagner model in Fig. 13 is closer to the experiments compared to the other models. As discussed earlier, the existence of the non-constant entry velocity terms in the Wagner (1932) model (Eq. 2) makes this model more accurate to account for the loss of speed in free-fall water entry. This justifies that such a model, in which the non-entry velocity terms are maintained could potentially predict the better pressure data for the free-fall wedge water entry than other models. Investigation into inclusion of the acceleration term in the other models will be conducted in a later study as part of this work.

Corrected Armand & Cointe Model

Although the peak magnitudes and their location are fairly reconstructed using the Armand & Cointe model (Fig. 9), one can observe from Figs. 6 and 7 that as the time passes, the residual pressure ($x << x_{sp}$) deviates considerably from the experimental results. For example, Fig. 8b shows that the residual pressure data at $x = 2$ cm reconstructed from Armand & Cointe method is 10.6 kPa, which is 140% higher than the experimental measured pressure, 4.4 kPa. This deviation, which comes from the assump-

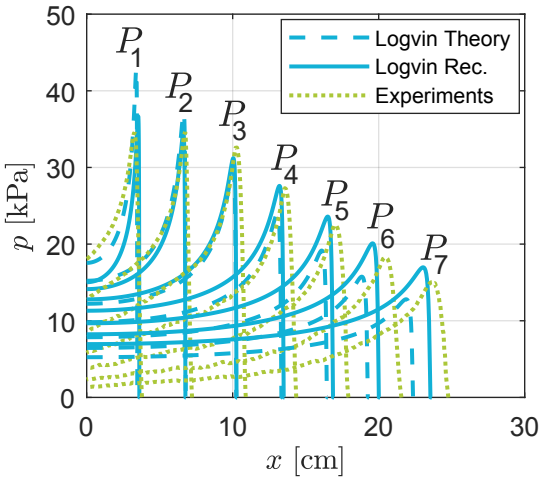

Figure 11: Spatial pressure distribution resulted from the traditional (theory) and the reconstruction approach using the Logvinovich (1969) model for $V_0 = 2.175$ m/s. Results are compared with the experimental pressure distribution. The curves correspond to the time steps that were presented in the Fig. 7.

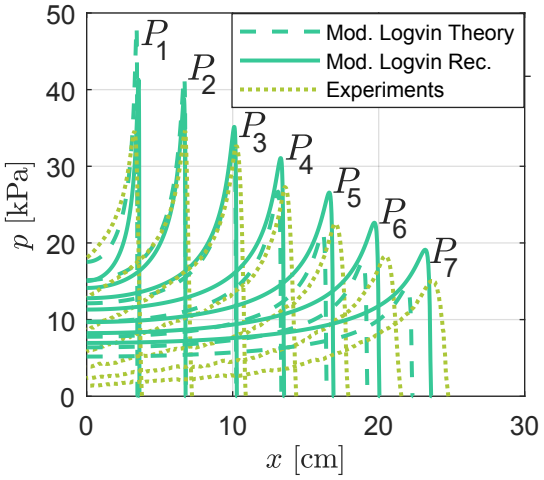

Figure 12: Spatial pressure distribution resulted from the traditional (theory) and the reconstruction approach using the Modified Logvinovich (1969) model for $V_0 = 2.175$ m/s. Results are compared with the experimental pressure distribution. The curves correspond to the time steps that were presented in the Fig. 7.

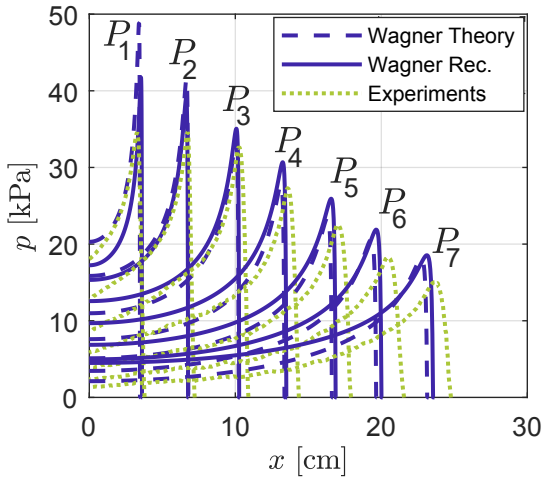

Figure 13: Spatial pressure distribution resulted from the traditional (theory) and the reconstruction approach using the Wagner (1932) model for $V_0 = 2.175$ m/s. Results are compared with the experimental pressure distribution. The curves correspond to the time steps that were presented in the Fig. 7.

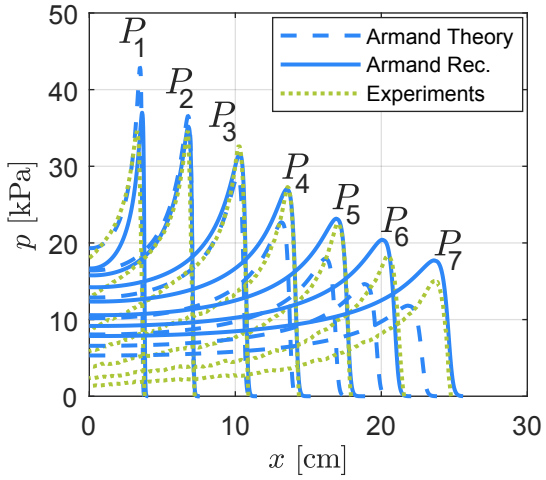

Figure 14: Spatial pressure distribution resulted from the traditional (theory) and the reconstruction approach using the Armand and Cointe (1986) model for $V_0 = 2.175$ m/s. Results are compared with the experimental pressure distribution. The curves correspond to the time steps that were presented in the Fig. 7.

tions that are used in the original model of Armand & Cointe, i.e. the constant entry velocity assumption, can drastically cause the hydrodynamic force to be over-predicted. To compensate for this deviation, a simple correction is applied to the formulation of the Armand and Cointe (1986) model. This modification is suggested for the outer domain by multiplying a correction term to the Eq. 6:

$$P_{modified\ out} = (1 - 3X_{sp} + 3X)\ P_{original\ out}. \tag{10}$$

This modification is made in a way that it preserves the location and the magnitudes of the peak as it is predicted in the original model. However, the residual pressure is adjusted so that it decreases over time as it does in the experiments. It should be noted that this modification is not physics-based and is based on the observation of the results and the comparisons. In the future, the authors would try to re-derive the theoretical formulations for the pressure distribution based on a free-fall water entry so that the corresponding terms for the non-constant entry velocity would remain in the pressure formulations.

Fig. 15(a) illustrates the reconstructed pressure distribution from corrected Armand & Cointe compared with the original reconstruction model and the experiments for $V_0 = 2.175$ m/s. The comparison shows that while the magnitude and the location of the peaks are maintained from the original reconstruction method, the corrected Armand & Cointe model reconstructs the residual pressure more accurately when compared to the experimental observations. For instance, Fig. 15(b) reveals that the deviation between reconstructed and experimental pressure at $x = 2$ cm reduces from 140% to 15% at $t = 19.5$ ms.

Pressure Time-Histories

The hydrodynamic pressure measured in the Javaherian et al. (2019) experiment were at single points. The pressure-time history for $H = 25.4$ cm is depicted in Fig 16 along with the reconstructed pressure-time histories from the original and modified Armand & Cointe reconstruction methods. The curves from left to the right denote the pressure history at the location of the sensors P_1 to P_7, respectively (see Fig. 3). For the period prior to the peak pressure, the modified and original Armand & Cointe models reconstruct the pressure time-history identically. The residual pressure data from the modified Armand & Cointe model matches very well with the experimental results compared to the original model.

Figs. 17 and 18 show the pressure-time history of the wedge reconstructed from modified Armand & Cointe method for drop heights of $H = 7.9$ and $H = 50.8$ cm, respectively. Results are compared with those of experimental measurements for each drop height. The comparison shows that the pressure-history for these drop heights are predicted well using this model. Compared with other sensors, the maximum deviation between the peak and residual pressure data is observed for the last two sensors. As discussed previously, these deviations are attributed to the

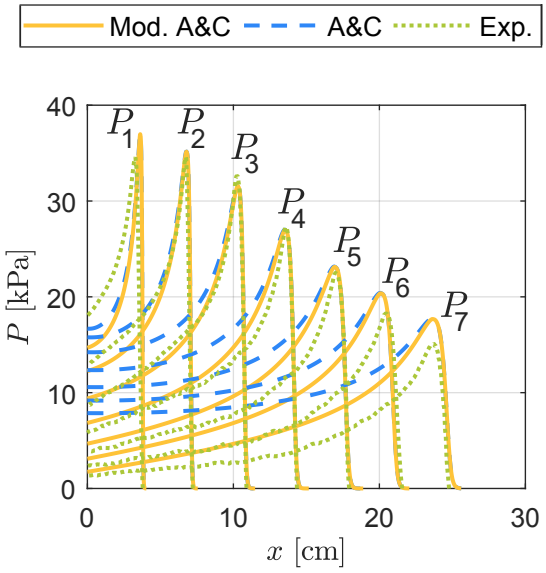

(a)

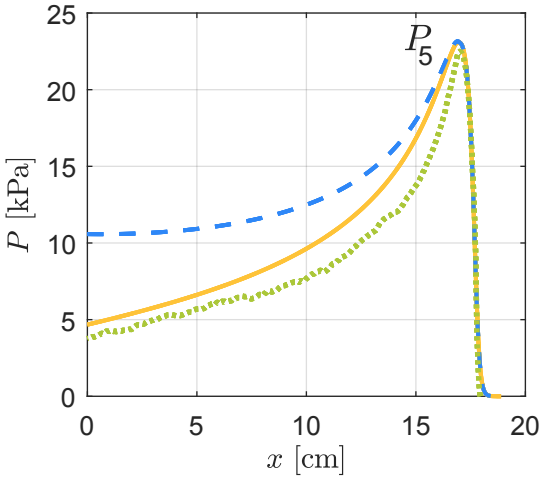

(b)

Figure 15: Comparison between the pressure distribution reconstructed from modified and original Armand & Cointe with experiments for the impact velocity of V_0 = 2.175 m/s.

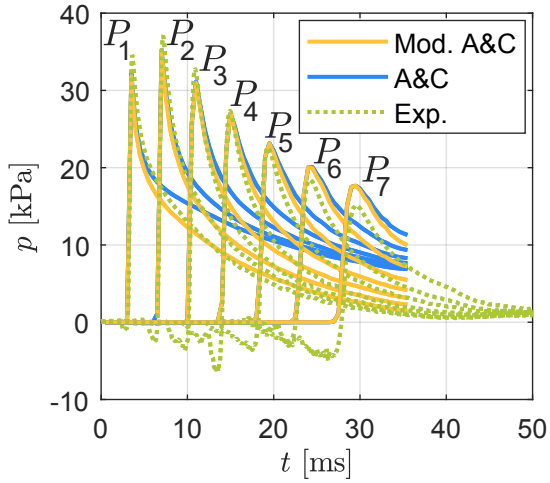

Figure 16: Pressure-time history reconstructed from modified Armand & Cointe model compared with the experimental results for H = 25.4 cm, V_0 = 2.175 m/s.

assumption of the constant entry velocity of the model. With the derivation of the physics-based modified formulation for the free-fall water entry, these deviations are expected to be reduced since the reduction of the pressure due to the loss of entry velocity would be more realistically captured.

Reconstructed Kinematics

To reconstruct the kinematics of the wedge, the force that exerts on the body during water entry is computed from the pressure-spatial distribution. Given the force-time history, the acceleration-, velocity- and position-time history can be obtained, subsequently. The kinematics of the wedge reconstructed from the modified Armand & Cointe model is reported in Fig. 19 for the impact velocity of V_0 = 2.175 m/s. Since the kinematics are reconstructed using experimental spray root data, they are plotted until the chine-wetted moment.

The vertical acceleration of the wedge reconstructed from the modified Armand & Cointe method is illustrated in Fig. 19(a) along with the experimental measurements. The acceleration starts with a negative value of -8.6 m/s^2, which is close to the gravitational acceleration of the falling body. The wedge experiences a sharp rise in the acceleration following the impact moment and reaches the maximum of acceleration of 40.12 m/s^2 at t = 18 ms. This magnitude is 10% higher than the corresponding experimental peak for the acceleration. This deviation is attributed to the 3D effects in the experiments, which is not resolved in the reconstruction process. In experiments, the 3D effects cause the pressure wave to be smaller at the sides of the wedge along the length compared to the pressure at the midspan of the wedge, say characteristic line (line x in Fig. 3). In the 2D reconstruction process, the pressure wave is assumed to be constant along the length of the wedge. This assumption

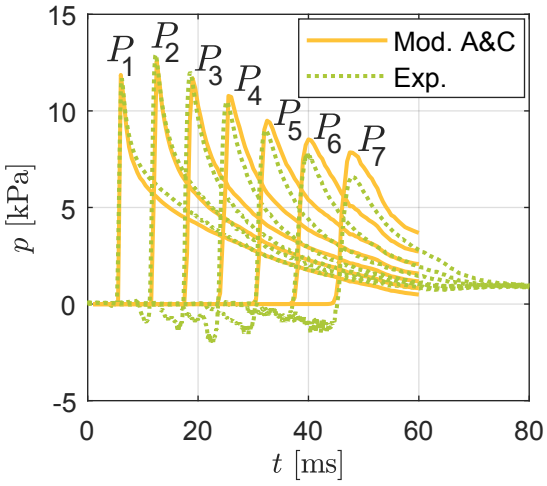

Figure 17: Pressure-time history reconstructed from modified Armand & Cointe model compared with the experimental results for $H = 7.9$ cm, $V_0 = 1.219$ m/s.

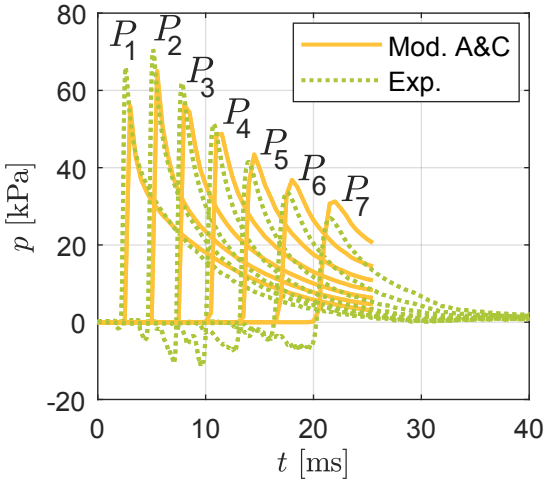

Figure 18: Pressure-time history reconstructed from modified Armand & Cointe model compared with the experimental results for $H = 50.8$ cm, $V_0 = 3.057$ m/s.

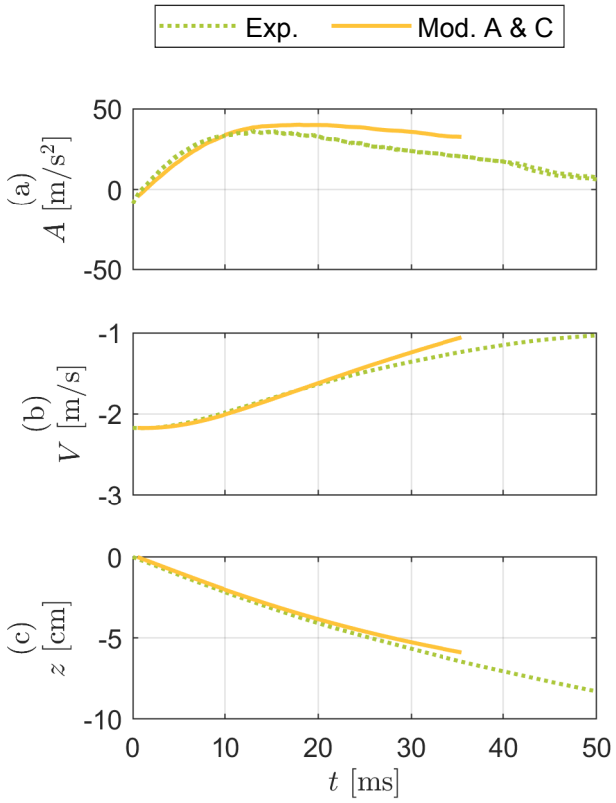

Figure 19: (a) Acceleration, (b) velocity and (c) position of the wedge reconstructed from Modified Armand & Cointe model for$V_0 = 2.175$ m/s. Results are compared with the experimental measurements.

would lead to compute a higher force in the reconstruction technique compared to the experiments. As the time increases, this deviation becomes larger. Hence, the reconstruction acceleration have a good agreement with the experimental measurements.

The vertical velocity of the wedge is shown in Fig. 19(b). The reconstructed velocity that starts with the impact velocity of 2.175 m/s, matches very well with the experiments for most of the time. Considering the hydrodynamic force due to impact, the magnitude of the velocity decreases tangibly as the wedge penetrates into the water. As the time passes, the reconstructed velocity decreases a little bit compared to the experimental results. Again, this is caused by the influence of the 3D effects on the acceleration curve. In fact, the higher upward (positive) acceleration, would cause the wedge to proceed slower downward.

Lastly, Fig. 19(c) depicts the vertical position-time history of the wedge for the impact velocity of $V_0 = 2.175$ m/s. As the wedge penetrates into the water, the position curve is nearly linear. The comparison shows a very good agreement between reconstructed position and the experiments except the small deviation at the final time steps.

CONCLUSIONS

In this paper, a reconstruction approach was proposed to estimate the hydrodynamic loading and kinematics of the wedge during water entry. This approach incorporates the spray root measurements into the traditional theoretical models. In fact, the spray root location is used as the input for the traditional theoretical models to reconstruct the hydrodynamic pressure and kinematics. This approach was evaluated by studying free-fall water entry of a rigid wedge with different impact velocities. A set of experiments conducted by Javaherian et al. (2019) was considered as the case study. The experimental spray root propagation was used to reconstruct the pressure distribution using five different theoretical models. Results were then compared with the experimental pressure measurements. The comparison showed that the reconstructed pressure using Armand & Cointe model has the best prediction for the location and magnitude of the peak pressure. For most time steps, the location and the magnitude of the peaks were predicted within 1.5% and 10% of error, respectively. However, the residual pressure (pressure at $x << x_{sp}$) was not well resolved with this model and could fall up to 140% higher than the experiments. This is attributed to the fact that the Armand & Cointe is based on the constant entry assumption and thus, it does not proportionately capture the loss of the pressure due to the reduction in the speed during the entry.

On the other hand, reconstructed pressure from the Wagner model could capture the residual pressure data more accurately. Since this model accounts for the change of the speed in the pressure formulation, it can better predict the residual pressure in a free-fall water entry. However, the prediction of the peak pressure from this model was more deviated from the experiments. The comparison showed that the prediction for the peak magnitude and its location by this model possess the errors of 15% and 2% for most of the time steps.

To improve the reconstruction results from the Armand & Cointe model and account for the loss of the velocity in the free-fall water entry, a correction term was proposed based on the observation and the comparison between reconstructed and experimental results. This term was defined in a way to implement the reduction in the residual pressure, while it does not influence the location and magnitude of the peak. Results showed that the maximum error in the prediction of the residual pressure could drop to 15% for the corrected Armand & Cointe model. A more physics-based model will be derived in future so that the non-constant entry terms would be maintained in the formulations.

To verify the proposed reconstruction approach, the study was repeated for the case study using the traditional theoretical models (pure theory). The computed pressure distribution from traditional approach were then compared with those of the reconstruction approach. The comparison demonstrated that the reconstruction approach could predict the peak magnitudes better than the pure theory. As an instance, the error of estimating the first peak, corresponding to P_1 for the experiments, could improve from 32% for the pure Wagner (1932) theory to 12% for the reconstructed Wagner model. The error of the location in which the peak occurs were also enhanced from within 8% for the traditional approach to 2% using the reconstruction approach.

It was also shown that the reconstruction approach can appropriately predict the kinematics of the wedge. Acceleration, velocity and the position of the wedge reconstructed from the Armand & Cointe model were compared with the experimental results that showed a good agreement. There are small deviations at the final time steps that were mainly caused by the 3D effects in the experiments.

This proposed reconstruction approach will be extended in future to take into account the structural response. The current study was the first step to develop this technique for predicting the hydrodynamics and structural response in water entry of highly-flexible structures.

ACKNOWLEDGEMENTS

Funding Statement: This work is funded by ONR Grant# N00014-20-1-2254 and NSF CBET Grant # 1944614. The authors gratefully acknowledge this support.

REFERENCES

Armand, J. L. and R. Cointe (1986). Hydrodynamic impact analysis of a cylinder. In *International offshore mechanics and arctic engineering. Symposium. 5*.

Faltinsen, O. (2005). *Hydrodynamics of high-speed marine vehicles*. Cambridge University Press.

Fisher, R. D., J. N. Gilbert, C. M. Gilbert, et al. (2019). A semi-theoretical method of estimating pressure & structural response on a flexible wedge. In *SNAME Maritime Convention*. The Society of Naval Architects and Marine Engineers.

Javaherian, M. J., Z. Ren, C. M. Gilbert, et al. (2019). Flow visualization, hydrodynamics, and structural response of a flexible wedge in water entry experiments. In *SNAME Maritime Convention*. The Society of Naval Architects and Marine Engineers.

Judge, C., A. Troesch, and M. Perlin (2004). Initial water impact of a wedge at vertical and oblique angles. *Journal of Engineering Mathematics 48*(3-4), 279–303.

Korobkin, A. (2004). Analytical models of water impact. *European Journal of Applied Mathematics 15*(6), 821—838.

Korobkin, A., R. Gueret, and Š. Malenica (2006). Hydroelastic coupling of beam finite element model with wagner theory of water impact. *Journal of Fluids and Structures 22*(4), 493–504.

Lewis, S. G., D. A. Hudson, S. R. Turnock, and D. J. Taunton (2010). Impact of a free-falling wedge with water: synchronized visualization, pressure and acceleration measurements. *Fluid Dynamics Research 42*(3), 035509.

Logvinovich, G. (1969). Hydrodynamics of flows with free boundaries.

Mei, X., Y. Liu, and D. K. Yue (1999). On the water impact of general two-dimensional sections. *Applied Ocean Research 21*(1), 1–15.

Panciroli, R. and M. Porfiri (2015). Analysis of hydroelastic slamming through particle image velocimetry. *Journal of Sound and Vibration 347*, 63 – 78.

Qin, Z. and R. Batra (2009). Local slamming impact of sandwich composite hulls. *International Journal of Solids and Structures 46*(10), 2011–2035.

Ren, Z., M. J. Javaherian, Z. Wang, C. Judge, F. Stern, and C. Ikeda-Gilbert (2018). Structural response due to the hydroelasticity of a slamming impact of a small craft in waves. In *32nd Symposium on Naval Hydrodynamics*.

Ren, Z., J. Javaherian, and C. Gilbert (2019). Vertical wedge drop experiments as a model for slamming. SNAME Maritime Convention, Tacoma, WA, USA, 29 October to 1 November 2019.

Shams, A., S. Zhao, and M. Porfiri (2017). Hydroelastic slamming of flexible wedges: Modeling and experiments from water entry to exit. *Physics of Fluids 29*(3), 037107.

von Karman, T. (1929). The impact of seaplane floats during landing. In *NACA TN 321, Washington, D.C., Oct.*

Vorus, W. S. (1996). A flat cylinder theory for vessel impact and steady planing resistance. *Journal of ship research 40*(02), 89–106.

Wagner, H. (1932). The landing of seaplanes. Technical Report Technical Note 622, 254, NACA.

Yettou, E., A. Desrochers, and Y. Champoux (2006). Experimental study on the water impact of a symmetrical wedge. *Fluid Dynamics Research 38*.

Zhao, R. and O. Faltinsen (1993). Water entry of two-dimensional bodies. *Journal of Fluid Mechanics 246*, 593–612.

Zhao, R., O. Faltinsen, and J. Aarsnes (1996). Water entry of arbitrary two-dimensional sections with and without flow separation. In *Proceedings of the 21st symposium on naval hydrodynamics*, pp. 408–423.

AUTHOR BIOGRAPHIES

Zhongshu Ren is a PhD candidate in the Kevin T. Crofton Department of Aerospace and Ocean Engineering at Virginia Polytechnic Institute and State University. Mr. Ren received his Bachelors degree from Tianjin University in Ocean Engineering in 2014. His PhD program is "Hydroelasticity of High-Speed Planing Craft Subject to Slamming Events" under the mentorship of Dr. Christine Gilbert. This program is primarily to help develop better design criteria for high-speed small craft operating in waves. He is the recipient of the David A. O'Neil Scholarship from SNAME in 2016 and the first place winner of the ASNE Graduate Poster Competition at TSS in 2017.

M. Javad Javaherian is a PhD candidate in the Kevin T. Crofton Department of Aerospace and Ocean Engineering at Virginia Polytechnic Institute and State University. He received his bachelor in Marine Engineering and Naval Architecture from Persian Gulf University of Iran. Mr. Javaherian also holds a Master's degree in Naval Architecture from Amirkabir University of Technology of Iran. His PhD research, supervised by Professor Christine Gilbert, is established on an experimental investigation on the effects of hydroelasticity on hydrodynamics and structural response of high-speed craft due to slamming. He is interested in fluid visualization, image processing, and digital image correlation technique to study the Fluid-Structure Interaction problems. Mr. Javaherian is a member of the American Society of Naval Engineers (ASNE) and the Society of Naval Architects and Marine Engineers (SNAME).

Dr. Christine Gilbert (née Ikeda) has been an assistant professor in the Kevin T. Crofton Department of Aerospace and Ocean Engineering at Virginia Polytechnic Institute and State University since 2016. She received her PhD (2012), Masters (2010), and Bachelors (2006) degrees from the University of Maryland in Mechanical Engineering. She has previously held appointments at the U.S. Naval Academy (2012 to 2014) and the University of New Orleans (2014 to 2016). Her research interests include experimental fluid-structure interaction as related to Ocean and Naval vessels and problems that involve impulsive loading. Dr. Gilbert's research group is currently developing new methods for performing non-traditional tow tank experiments for slamming of small craft in waves. She has authored/co-authored over 20 journal and conference papers on fluid-structure interaction and small vessel slamming. She was a recipient of an ONR Young Investigator Program grant in 2015 and the NSF Career Award in 2020.